Environmental Science and Pollution Research
https://doi.org/10.1007/s11356-020-08025-7

WASTE AND BIOMASS MANAGEMENT & VALORIZATION

Influence of addition of organic fillers on the properties of mechanically recycled PLA

Freddys R. Beltrán[1,2] · Gerald Gaspar[1] · Masoud Dadras Chomachayi[3] · Azam Jalali-Arani[4] · Antonio A. Lozano-Pérez[5] · José L. Cenis[5] · María U. de la Orden[2,6] · Ernesto Pérez[7] · Joaquín M. Martínez Urreaga[1,2]

Received: 30 October 2019 / Accepted: 6 February 2020

Abstract

Poly(lactic acid) (PLA) is one of the most used biobased and biodegradable polymers. Due to their high stability, some of the newest grades of PLA are only degradable under severe industrial conditions. For these grades, mechanical recycling is a viable end-of-life option, with great environmental advantages. However, the polymer undergoes degradation during its service life and in the melt reprocessing, which leads to a decrease in properties that can compromise the recyclability of PLA. The goal of this work was to evaluate the usefulness of adding small amounts of two organic fillers, chitosan, and silk fibroin nanoparticles, during the recycling process for improving the properties of the recycled plastic. The degradation level of the aged polymer and the nature and amount of filler affect the performance of the recycled plastics. The fillers reduce the degradation during the melt reprocessing of PLA previously subjected to severe hydrolysis, thus increasing the intrinsic viscosity of the recycled plastic. A careful selection of the added organic filler lead to recycled plastics with improvements in some key mechanical, thermal, and barrier properties. Thus, the use of organic fillers represents a cost-effective and environmentally sound way for improving the mechanical recycling of bioplastics.

Keywords Poly(lactic acid) · Mechanical recycling · Silk fibroin nanoparticle · Chitosan · Gas barrier properties · Mechanical properties · Thermal properties

Responsible editor: Angeles Blanco

✉ Joaquín M. Martínez Urreaga
joaquin.martinez@upm.es

[1] Dpto. Ingeniería Química Industrial y Medio Ambiente, Universidad Politécnica de Madrid, E.T.S.I. Industriales, 28006 Madrid, Spain

[2] Grupo de Investigación: Polímeros, Caracterización y Aplicaciones (POLCA, Associated Unit to CSIC), Madrid, Spain

[3] Mahshahr Campus, Amirkabir University of Technology, P.O. Box 63517-13178, Mahshahr, Iran

[4] Department of Polymer Engineering & Color Technology, Amirkabir University of Technology, P.O. Box 15875-4413, Tehran, Iran

[5] Dpto. Biotecnología, Instituto Murciano de Investigación y Desarrollo Agrario y Alimentario (IMIDA), 30150 Murcia, Spain

[6] Dpto. de Química Orgánica I, Facultad de Óptica y Optometría, Universidad Complutense de Madrid, 28037 Madrid, Spain

[7] Instituto de Ciencia y Tecnología de Polímeros, ICTP-CSIC, 28006 Madrid, Spain

Abbreviations

PLA	Poly(lactic acid)
SFN	Silk fibroin nanoparticles
SF	Silk fibroin
SEM	Scanning electron microscopy
DSC	Differential scanning calorimetry
TGA	Thermogravimetric analysis
WVTR	Water vapor transmission rate
HSFN	Silk fibroin nanoparticles obtained by acid hydrolysis
DSFN	Silk fibroin nanoparticles obtained by desolvation
FTIR	Fourier-transform infrared
ATR	Attenuated total reflectance
T_g	Glass transition temperature
T_{cc}	Cold crystallization temperature
T_m	Melting temperature
ΔH_{cc}	Cold crystallization enthalpy
ΔH_m	Melting enthalpy
X_c	Crystallinity degree
T_{10}	Temperature at which 10% of the mass
T_{max}	temperature of maximum degradation rate

Published online: 10 February 2020

Introduction

In recent years, the environmental problem generated due to the massive utilization of fossil fuel-based plastics, and the inadequate management of such wastes, has raised a fair amount of attention. Among the most important solutions posed to this problem is the progressive substitution of fossil-based plastics, in certain applications, with bioplastics such as PLA. PLA is an aliphatic polyester, produced via ring opening polymerization of lactide, a dimer of lactic acid obtained from the fermentation of carbohydrates present in corn, sugar cane, or potato (Castro-Aguirre et al. 2016). PLA is one of the most researched and used bioplastics, due to its biodegradability, biocompatibility, and acceptable mechanical and optical properties (Farah et al. 2016; Reddy et al. 2013). The production, and consumption, of PLA has grown steadily over the last years, exceeding the 200 kt in 2018 (Chinthapalli et al. 2019). Such increase could be attributed to the development of new grades with improved properties (Nagarajan et al. 2016), which allow using PLA in a wide range of applications such as food packaging and textile industry (Cecchi et al. 2019).

The utilization of PLA in applications typically related to fossil fuel-based polymers leads to a reduction in the consumption of nonrenewable feedstocks. However, PLA grades destined to demanding applications degrade at a very low rate and are compostable only in industrial conditions (Haider et al. 2018; Niaounakis 2019), which, in conjunction with an inadequate management of the wastes, could result in an important environmental problem. Furthermore, it cannot be ignored that the production of the feedstock used in the manufacture of PLA requires large amounts of croplands, which might end resulting in food supply and overpricing issues, especially in poorer countries (Mülhaupt 2013). Therefore, the development of environmentally friendly methods for the management of PLA wastes is crucial in the sustainability of this bioplastic. Among the potential valorization methods, mechanical recycling plays a prominent role, since several life cycle assessment studies point out that it allows to reduce the environmental impact by decreasing the emissions as well as the consumption of raw materials (Rossi et al. 2015; Soroudi and Jakubowicz 2013; Zhao et al. 2018).

Despite the environmental advantages of the mechanical recycling of PLA, a holistic approach of the recycling process is necessary to assure its feasibility. On the one hand, plastic recovery infrastructures should be adapted to allow the introduction of a separate stream for PLA. On the other hand, previous studies indicate that some crucial properties in packaging applications decrease during the mechanical recycling of the plastic (Beltrán et al. 2018a), which might negatively affect the market for the recycled PLA, and thus threaten the sustainability of the process. Consequently, it is necessary to develop economical and environmentally friendly methods that allow improving the performance of recycled PLA, increasing its attractiveness to the plastic transformers.

It has been reported in previous works that the use of additives during the mechanical recycling, such as functionalized clays (Beltrán et al. 2018c) or chain extenders and crosslinking agents (Beltrán et al. 2019), leads to a reduced degradation of the polymer, thus improving the properties of the recycled material.

Another potential alternative for improving the properties of recycled PLA is the utilization of organic fillers coming from renewable resources. This kind of fillers are very interesting due to their low cost, availability, and biodegradability. For example, Tesfaye et al. reported that silk fibroin (SF) nanocrystals have a nucleating effect on PLA and also help to diminish the reduction of the intrinsic viscosity during multiple reprocessing cycles (Tesfaye et al. 2017). In the same line, Patwa et al. reported that the addition of silk fibroin nano-discs to PLA led to an increase in crystallization and improvements in thermal stability, toughness, and gas barrier properties (Patwa et al. 2018). Other authors, such as Li et al., have added small amounts of functionalized chitosan to PLA, obtaining improvements on the Young modulus and tensile strength of the polymer (Li et al. 2019).

The previously mentioned studies point out that is possible to use organic fillers to improve the properties of PLA. However, there is very little data regarding the effect of organic fillers, concretely SFN and chitosan, on the structure and properties of postconsumer PLA subjected to mechanical recycling. *Bombyx mori* SF presents excellent biomechanical properties, including non-toxicity, slow biodegradation, and exceptional biocompatibility, making it an outstanding biomaterial for use in a wide range of applications (Omenetto and Kaplan 2010). SF is composed of two peptidic chains, namely, high molecular weight chain (H) and a low molecular weight chain (L) with ~ 325 kDa and ~ 25 kDa respectively, linked by a single disulfide bridge. The high molecular weight chain of SF is composed of repetitive crystalline connected by amorphous domains (Altman et al. 2003; Zhou et al. 2001). The extensive hydrogen bonding network of the SF, their hydrophobic nature, and high degree of crystallinity contribute to the stability of silk biomaterials and their outstanding mechanical properties (Altman et al. 2003).

Consequently, the main aim of this work is to study the effects of different organic fillers on the structure and on the thermal, mechanical, gas barrier, and optical properties of mechanically recycled PLA. In order to simulate the polymer degradation during its service life, two accelerated aging processes were carried out. Thus, a simulated postconsumer PLA was obtained by subjecting the starting granulated PLA to (i) a melt compounding and compression-molding step, (ii) an accelerated aging process comprising hydrothermal and photochemical degradation steps, and (iii) a demanding washing step. In a parallel way, severely degraded PLA was obtained

by hydrolytic degradation of the starting granulate at 60 °C for 5 days. Then, both postconsumer and hydrolyzed PLA were melt compounded along with the SFN and chitosan, compressed molded into films and characterized by SEM, solution viscosimetry, microhardness measurements, DSC, TGA, gas permeability, and WVTR measurements.

Materials and methods

Materials

Ingeo™ 2003D, a commercial grade of PLA with a melt mass-flow rate of 6 g/10 min (2.16 kg at 210 °C), was used. *Bombyx mori* silkworm cocoons were obtained from the University of Guilan (Iran) and from IMIDA (Spain). Sodium carbonate (Na_2CO_3) and chloroform were purchased from Merck. Sulfuric acid (96% purity) was supplied by Honeywell. High molecular weight chitosan (HCh, M_w 100–300 kDa) was supplied by Acros Organics, and low molecular weight chitosan (LCh, M_v 50–150 kDa) was supplied by Sigma-Aldrich.

Preparation of SFN

The first obtaining process is based in that published by Tao et al. (Tao et al. 2012). In this process, *Bombyx mori* cocoons were boiled twice for 30 min in an aqueous solution of Na_2CO_3 (0.5% *w*/*v*) at 98 °C, followed by washing several times with distilled water to remove impurities and sericin. After the degumming step, silk fibroin nanoparticles were prepared using two different methods. In one process, the degummed silk fibroin (SF) was dried overnight at 50 °C and then hydrolyzed in an aqueous solution of H_2SO_4 (64 wt%) at 45 °C under continuous stirring. The reaction was stopped by adding 50 ml of distilled water after 2 h. The ratio between SF and H_2SO_4 solution was 1:10. The mixture was then centrifuged at 5000 rpm for 15 min to reach a neutral pH. Finally, the silk fibroin hydrolysate was dialyzed in a cellulose membrane tube (molecular weight cutoff 3.5 kD) against distilled water for 4 days, and the pelleted portion was freeze-dried, for 48 h, to obtain the dry SFN, labeled as HSFN.

The second process is based in a previously published desolvation method (Lozano-Pérez et al. 2017). Briefly, degummed silk fibroin was dissolved in Ajisawa's solvent system at 65 °C for 3 h (Ajisawa 1998), filtered, and dialyzed for 48 h against distilled water with several changes in order to remove salt and alcohol. Nanoparticles were prepared by rapid desolvation of the freshly prepared SF aqueous solution in absolute ethanol. The resultant suspension was stirred for 2 h, and the particle suspension was recovered by centrifugation (12,000*g*, 15 min, 8 °C). Nanoparticles were repeatedly washed (three times) with ultrapure water and finally dispersed in ultrapure water by using high power ultrasounds for 1 min at 10% of amplitude in a Branson Digital Sonifier SFX 550 equipped with a 1/8″ tapered microtip (Branson Ultrasonics Corp, Danbury). Finally, the nanoparticles were freeze-dried for 72 h to obtain the SFN, labeled as DSFN.

Preparation of the samples

Scheme 1 summarizes the process followed for the aging of PLA and subsequent preparation of the recycled PLA-based materials. Two different aging processes were used to consider different levels of degradation in PLA wastes. In the first process, a simulated postconsumer PLA was obtained by subjecting the starting granulated PLA to an extrusion process in a Rondol Microlab twin-screw extruder (L/D = 20), at 60 rpm and with a temperature profile from hopper to die: 125, 160, 190, 190, and 180 °C. The obtained material was compressed molded into films (200 ± 10 μm) at 190 °C, using an IQAP-LAP hot plate press. The films (PLAV) were then subjected to an accelerated aging comprising 40 h of photochemical degradation in an Atlas UVCON chamber, equipped with eight F40UVB lamps; 468 h of thermal degradation at 50 °C in an oven; and 240 h of hydrolytic degradation at 25 °C in demineralized water. Finally, the aged material was washed for 15 min, at 85 °C in an aqueous solution of NaOH (1.0 wt%) and a surfactant (Triton X, 0.3 wt%), as it has been suggested in previous studies (Beltrán et al. 2019). In the second process, the starting granulated PLA was immersed in demineralized water at 60 °C for 5 days to obtain a severely degraded PLA (hydrolyzed PLA).

After the different aging processes, both hydrolyzed and postconsumer PLA were extruded in conjunction with four different organic fillers: HSFN, DSFN, and chitosan (of high and low molecular weight). The nanoparticles were added in a proportion of 1 wt%, while the chitosan was added in a proportion of 1 and 5 wt%. Finally, the recycled materials were transformed into films (200 ± 10 μm) by compression molding. The obtained materials are summarized in Table 1.

Characterization techniques

Intrinsic viscosity of the different materials was measured following the ISO 1628 standard, using an Ubbelohde viscometer at 25 °C and chloroform as the solvent. The measurements were made at four different concentrations.

A Type M Shimadzu microhardness tester was used to measure the Vickers hardness of the different samples according to ASTM E384. A Vickers pyramidal indenter was used to apply a load of 25 g during 10 s. Each sample was measured six times.

FTIR spectra of the different samples were recorded with a Nicolet iS10 spectrometer, equipped with a diamond ATR accessory. Sixteen scans and a 4-cm^{-1} resolution were used.

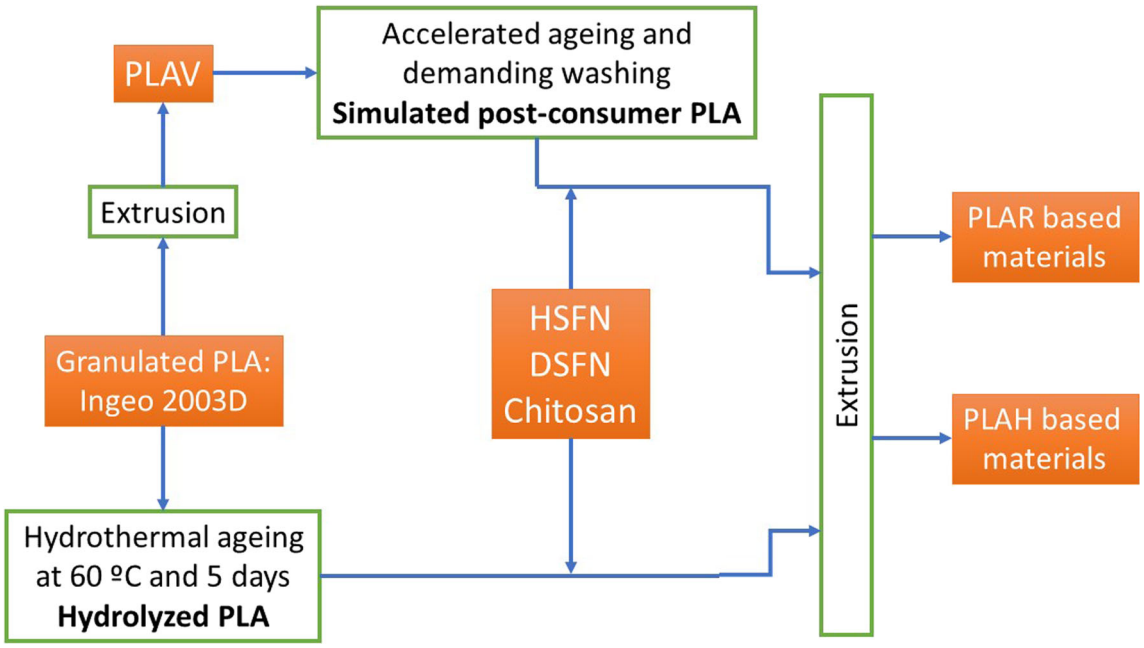

Scheme 1 Preparation of the different samples

DSC scans of the different materials were performed in a TA Instruments Q20 calorimeter, under nitrogen atmosphere (50 mL/min). Samples of around 5 mg were placed in aluminum pans, heated from 0 to 180 °C, and kept at 180 °C for 3 min. Subsequently, the samples were cooled to 0 °C, kept at 0 °C for 1 min, and, finally, heated again to

Table 1 Materials obtained after the recycling process

Sample	Description
PLAV	PLA film made by extrusion and compression molding of granulated PLA
PLAR	PLA film made by extrusion and compression molding of simulated postconsumer PLA
PLAH	PLA film made by extrusion and compression molding of hydrolyzed PLA
PLAR-1HSFN	PLA film made by extrusion and compression molding of simulated postconsumer PLA and 1% of silk fibroin nanoparticles obtained via hydrolysis
PLAH-1HSFN	PLA film made by extrusion and compression molding of hydrolyzed PLA and 1% of silk fibroin nanoparticles obtained via hydrolysis
PLAR-1DSFN	PLA film made by extrusion and compression molding of simulated postconsumer PLA and 1% of silk fibroin nanoparticles obtained via desolvation method
PLAR-2DSFN	PLA film made by extrusion and compression molding of simulated postconsumer PLA and 2% of silk fibroin nanoparticles obtained via desolvation method
PLAH-1DSFN	PLA film made by extrusion and compression molding of hydrolyzed PLA and 1% of silk fibroin nanoparticles obtained via desolvation method
PLAR-1LCh	PLA film made by extrusion and compression molding of simulated postconsumer PLA and 1% of low molecular weight chitosan
PLAR-5LCh	PLA film made by extrusion and compression molding of simulated postconsumer PLA and 5% of low molecular weight chitosan
PLAH-1LCh	PLA film made by extrusion and compression molding of hydrolyzed PLA and 1% of low molecular weight chitosan
PLAH-5LCh	PLA film made by extrusion and compression molding of hydrolyzed PLA and 5% of low molecular weight chitosan
PLAR-1HCh	PLA film made by extrusion and compression molding of simulated postconsumer PLA and 1% of high molecular weight chitosan
PLAR-5HCh	PLA film made by extrusion and compression molding of simulated postconsumer PLA and 5% of high molecular weight chitosan

180 °C. All the scans were performed at a heating or cooling rate of 5 °C/min.

The thermal stability of the samples was studied by means of TGA, which was conducted in a TA Instruments TGA2050 thermobalance, using 10 mg samples, under nitrogen atmosphere (30 mL/min). The samples were heated from room temperature to 800 °C at 10 °C/min.

The permeability against oxygen was measured following the ISO 2782 standard in a homemade permeation cell, at 30 °C and with a gas pressure of 1 bar. WVTR of the different samples was measured according to the ISO 2528 standard. Thin films (9 ± 2 μm) of the different materials were prepared by casting (0.1 g of polymer/10 ml of chloroform). The permeability cups were filled with 2 g of dry silica gel, sealed with the sample film, and placed in a 90% relative humidity atmosphere at 23 °C. The cups were weighed after different exposure times. *WVTR* (g/day·cm^2) was determined using Eq. 1:

$$WVTR = \frac{240*(m_t - m_0)}{A*t} \quad (1)$$

where m_t is the mass of the cup at time t, m_0 is the initial mass of the cup, and A is the exposed area of the film. Each sample was measured three times.

Results and discussion

Morphology of the PLA-based materials

The filler dispersion plays a prominent role in key properties of PLA-based materials, such as intrinsic viscosity, hardness, and gas barrier properties. Therefore, it is important to determine the dispersion of the different organic fillers (Fig. 1), in order to obtain recycled materials with improved properties and, thus, more attractive to the plastics market. The dispersion of the different fillers in the PLA matrix was studied using scanning electron microscopy. Figure 2 a–d correspond to the different PLA samples filled with HSFN and DSFN. Overall, silk fibroin nanoparticles (diameter < 500 nm) show a good dispersion in the PLA matrix. This behavior could be attributed to the hydrophobic character of the silk fibroin, which increases the compatibility with a hydrophobic matrix, such as PLA, thus facilitating the dispersion of the nanoparticles (Patwa et al. 2018; Tesfaye et al. 2017). Furthermore, the –NH and –OH groups present in the structure of SFN (Fig. 1) might interact with the terminal –COOH and –OH groups existing in both postconsumer and hydrolyzed PLA (Beltrán et al. 2018b), thus improving the compatibility between both materials. However, some aggregates bigger than 1 μm were observed, especially in the samples with DSFN (Fig. 2d). To better understand this behavior, it is necessary to analyze the chemical structure of the nanoparticles by means of FTIR-ATR.

Figure 3 shows the FTIR-ATR spectra of both HSFN and DSFN. As it could be expected, the spectra of both samples are very similar, showing the typical absorption bands around 1630, 1520, and 1230 cm^{-1} that correspond to amide I, amide II, and amide III, respectively. However, it is worth to note that there are some slight differences between the spectra of both nanoparticles. In DSFN, the amide I band is displaced toward lower wavenumbers, and the amide III band shows a small shoulder at 1267 cm^{-1}. Both changes are related to the transformation from a random coil structure, named silk I, to a better organized sheet structure known as silk II (Tao et al. 2012; Tesfaye et al. 2017). The presence of a more ordered structure might result in stronger molecular interactions inside the DSFN nanoparticles via hydrogen bonding between the –NH and –OH groups present in the structure of silk fibroin (Fig. 1). Such interactions favor the formation of aggregates and result in a poorer dispersion of the DSFN in the PLA matrix.

Regarding the behavior of the samples with chitosan, previous studies conducted by Li et al. (Li et al. 2019) and Suyatma et al. (Suyatma et al. 2004) point out that PLA and chitosan are immiscible, due to the hydrophilic nature of chitosan. Figure 2e shows that, despite there are some holes that indicate poor adhesion between phases, the dispersion of the high molecular chitosan is relatively good. To explain this behavior, one should consider the presence of carboxyl and hydroxyl end groups in recycled PLA. These groups might interact with the hydroxyl and amino groups present in chitosan (Fig. 1), thus improving the compatibility between the two polymeric phases.

Properties of the PLA-based materials

Intrinsic viscosity of the PLA-based materials

The intrinsic viscosity is one of the most important properties of polymers such as PLA and other polyesters, not only because of its relationship with molecular weight but also for the role it plays on the processing of the plastics. The industrial manufacturing processes are designed to operate at specific conditions, so that drastic changes in the intrinsic viscosity of recycled PLA might discourage the use of this plastic. The effect of the organic fillers on the intrinsic viscosity of PLA was measured by means of solution viscosimetry, and the results are presented in Fig. 4. It can be seen that the accelerated aging, washing, and reprocessing lead to a decrease of approximately 13% of the intrinsic viscosity of PLA. This phenomenon was previously studied (Beltrán et al. 2018b), and it can be attributed to the degradation processes that take place during the whole recycling process. Several chain

scission mechanisms are involved in the degradation of PLA during recycling, such as hydrolysis, oxidative random chain scission, and inter- and intramolecular transesterification (Cuadri and Martín-Alfonso 2018). On the other hand, PLAH presents a much lower intrinsic viscosity, less than 50% of the virgin polymer viscosity, thus showing the massive chain scission caused by the severe hydrolytic degradation to which the polymer was subjected.

Regarding the behavior of the samples filled with silk fibroin nanoparticles, Fig. 4 shows that the effect varies with both the type of nanoparticle and the level of degradation of PLA. For PLAR, the recycled polymer obtained from slightly degraded PLA, the nanoparticles obtained via acid hydrolysis seem to cause the degradation of PLA, while those obtained by the desolvation method do not significantly affect the intrinsic viscosity of the polymer. Tesfaye et al. (Tesfaye et al. 2017) and Patwa et al. (Patwa et al. 2018) reported a similar behavior in samples of PLA and silk fibroin nanoparticles obtained via acid hydrolysis. This behavior could be explained considering the presence of some residual acid groups in the nanoparticles, since it is known that acid groups can catalyze the degradation of PLA during melt processing (Auras et al. 2010). The different behavior of DSFN could be because this fibroin was obtained in the absence of sulfuric acid and also to the poor interaction between PLA and DSFN, as it was seen by means of SEM microscopy.

Figure 4 also shows that the PLAH samples containing silk fibroin nanoparticles present a different behavior than those of PLAR. In PLAH-based materials, the addition of both HSFN and DSFN led to important increases of the intrinsic viscosity, which could expand the applications of the recycled plastic. These results are rather surprising, since the presence of HSFN can catalyze the degradation of PLA during processing, as it has been shown above. However, it must be taken into account that, due to the severe hydrolytic degradation suffered, PLA has a large amount of terminal –COOH groups, which catalyze the subsequent degradation of PLA during the melt reprocessing step to obtain PLAH. The presence of fibroin nanoparticles during the reprocessing step could block, through acid-base interactions, a significant proportion of such –COOH groups, thus limiting their pernicious catalytic effect. Patwa et al. also observed that silk fibroin can limit the degradation of PLA during processing (Patwa et al. 2018). These authors pointed out that, in certain conditions, PLA and SFN could interact and form structures that delay the chain movement during processing, thus contributing to decrease the degradation of the polymer.

Moreover, the positive effect of the fibroin depends on the process of obtaining the nanoparticles. Again, the material reinforced with fibroin nanoparticles obtained by acid hydrolysis shows lower intrinsic viscosity, probably due to the

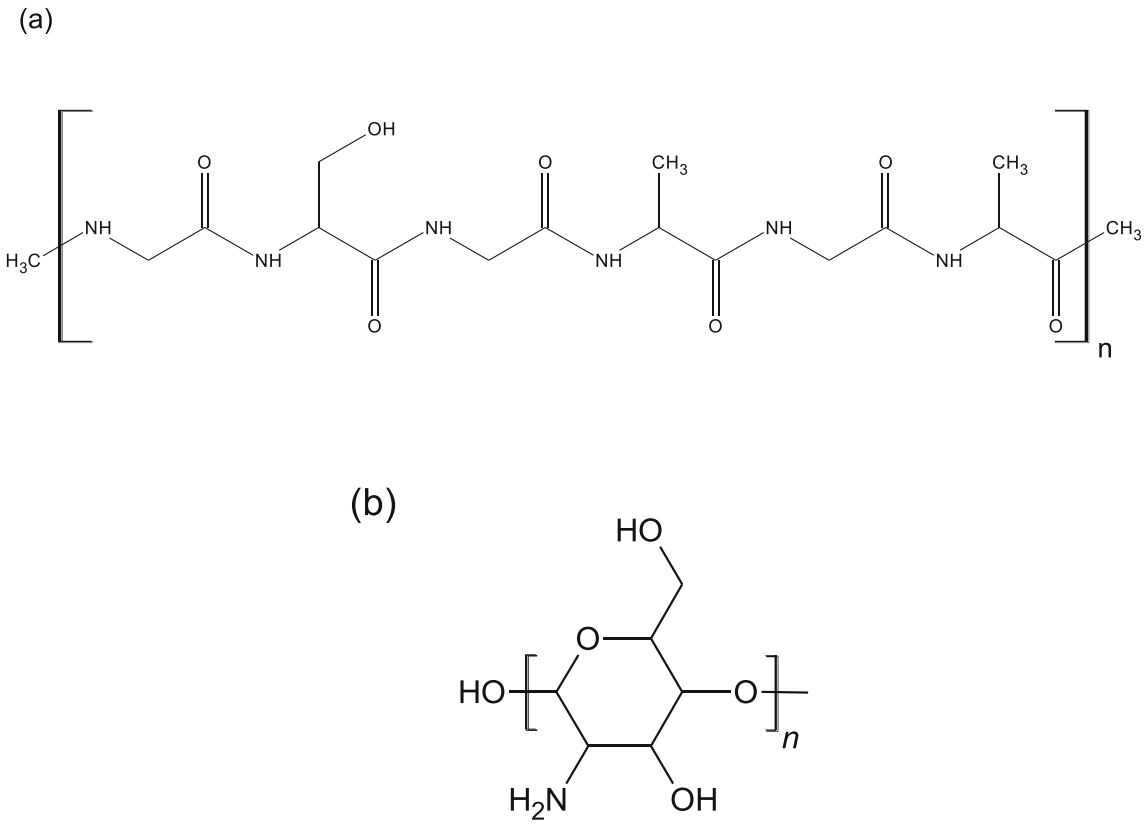

Fig. 1 Chemical structures of (**a**) silk fibroin and (**b**) chitosan

presence of some acid groups that catalyze the polymer degradation during the melt reprocessing.

Regarding the behavior of the samples with chitosan, Fig. 4 shows that the level of degradation of PLA and the molecular weight of chitosan play a very important role on the final intrinsic viscosity of the materials. The PLAR-1LCh sample presents no significant change of the intrinsic viscosity, while the rest of the PLAR-chitosan materials show lower values in comparison with PLAR (around 18%). The behavior of PLAR-1LCh could be explained by the low amount of chitosan and the poor interaction between PLA and this kind of chitosan. However, the reduced viscosity observed in the other composites of PLA and chitosan has not been fully explained, although Hijazi et al. (Hijazi et al. 2019) reported that higher amounts of chitosan nanoparticles could contribute to increase the shear stresses during the extrusion, resulting in further degradation of PLA.

The behavior of the PLAH samples is very different. The addition of chitosan led in these cases to an increase of the intrinsic viscosity, regardless of the concentration and molecular weight of chitosan, as opposed to the PLAR samples. As it was discussed for the PLAH samples reinforced with fibroin nanoparticles, this behavior could be due to the high amount of terminal –COOH groups present in the severely hydrolyzed

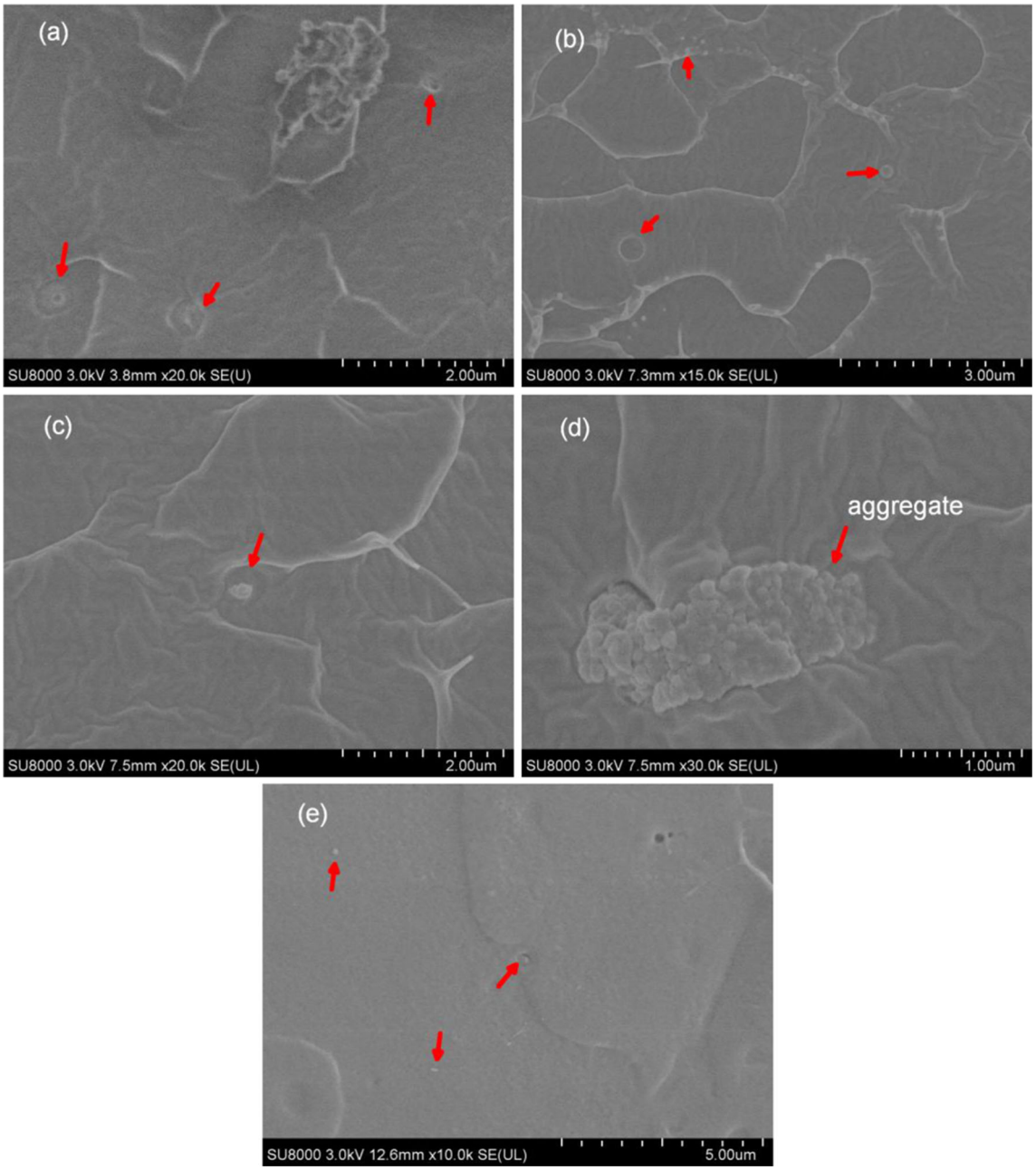

Fig. 2 SEM photographs of (**a**) PLAR-1HSFN, (**b**) PLAH-1HSFN, (**c**) and (**d**) PLAR-2DSFN and (**e**) PLAR-5HCh

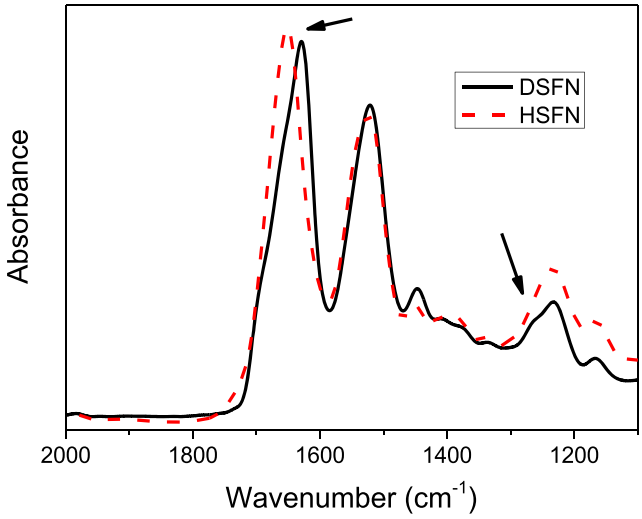

Fig. 3 FTIR-ATR spectra of the HSFN and DSFN

PLA. The amino groups existing in the structure of chitosan (Fig. 1) can block some of such terminal –COOH groups (Elsawy et al. 2017), thus reducing their catalytic effect on the degradation of the polymer during melt reprocessing. A similar result was obtained in a previous work by using amino-modified halloysite in the recycling of PLA (Beltrán et al. 2018c).

Thermal properties of the PLA-based materials

The properties, and hence the applications, of the recycled plastics depend on the thermal transitions and crystalline structures of the polymer. The effects of the different organic fillers on the thermal behavior of PLA, studied by means of DSC, are summarized on Fig. 5 and Table 2. It can be seen on Fig. 5a that virgin PLA shows a glass transition close to 60 °C, an exothermic peak corresponding to cold crystallization, between 105 and 110 °C, and a double melting endothermic peak over 140 °C. The presence of this double melting behavior has been reported in previous studies (Beltrán et al. 2018b; Di Lorenzo 2006) and is related to a melt recrystallization mechanism in which less perfect crystals melt at lower temperatures, rearrange into more ordered structures and thus melt at higher temperatures.

The mechanical recycling causes some differences in the thermal transitions of PLA. Firstly, it can be seen on both Fig. 5 and Table 2 that recycled PLA has a lower T_{cc} value than PLAV. This behavior could be attributed to the degradation of the polymer during the aging, washing, and reprocessing processes, since shorter polymer chains crystallize more easily. Secondly, it can be seen that the high temperature melting peak is more relevant in the recycled polymer, which can also be related to the presence of shorter polymer chains. These shorter polymer chains have increased mobility and can rearrange more easily into more perfect structures (Beltrán et al. 2016).

Regarding the behavior of the samples with organic fillers, Fig. 5 and Table 2 show that the use of organic nanofillers in the recycling process causes small displacements of T_{cc} toward lower values. This displacement, although small, could be an indicative of the nucleating effect of the nanoparticles on the crystallization of PLA. This result is in good agreement with those reported by other authors for virgin PLA reinforced with fibroin nanoparticles (Tesfaye et al. 2017) and chitosan (Elsawy et al. 2016). Anyway, the small differences observed in Table 2 in the values of T_{cc}, ΔH_{cc}, and ΔH_m point out that the nucleating effect of the organic nanoparticles is limited.

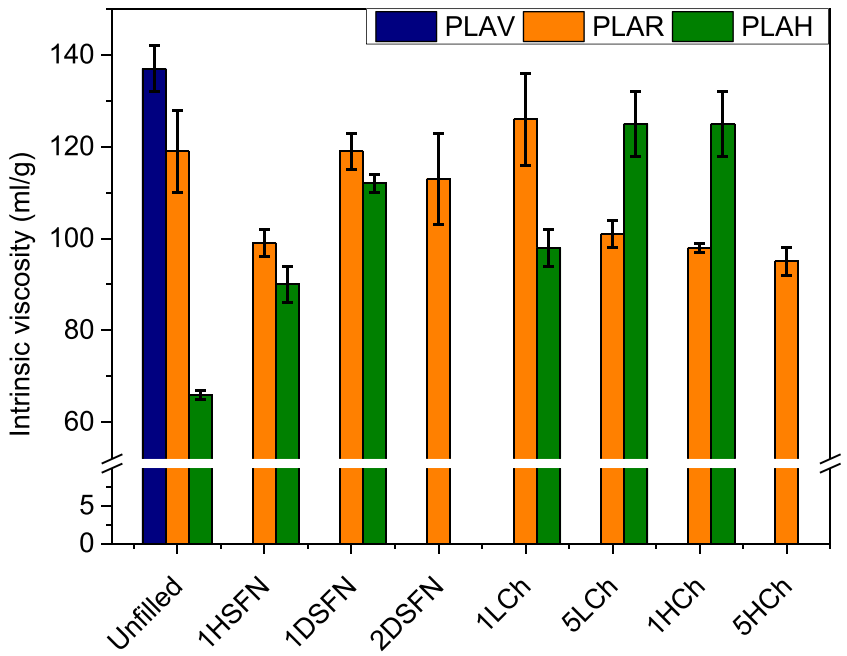

Fig. 4 Intrinsic viscosity of the PLA-based materials

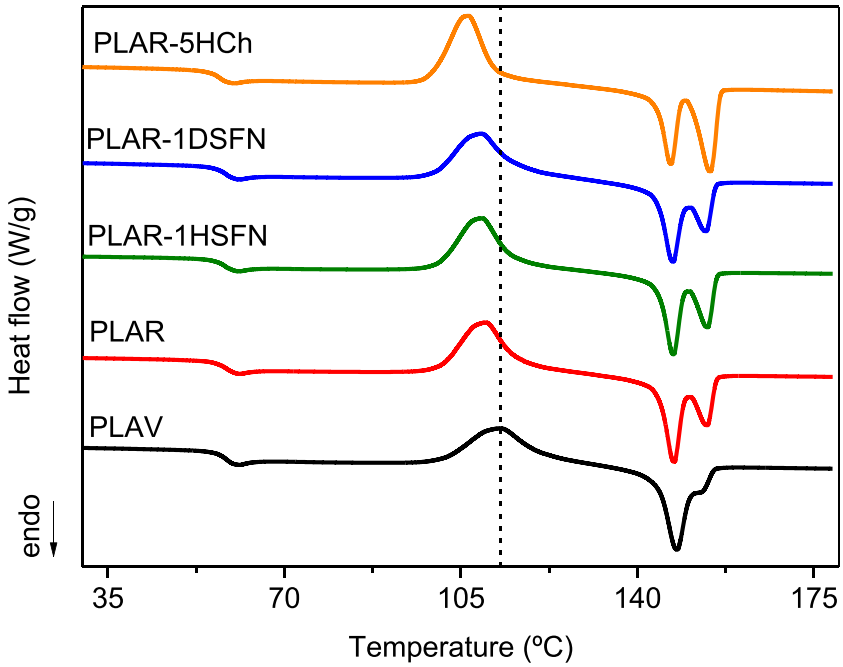

Fig. 5 DSC second heating scans of the PLA-based materials

As to the thermal stability, Table 3 summarizes the TGA characteristic temperatures of the different PLA samples. T_{10} and T_{max} are commonly used as an indicator of the thermal stability of the materials. Table 3 shows that mechanical recycling causes a decrease of the thermal stability of PLA. This result has been reported in previous studies, and it is related to the degradation of PLA during the aging and recycling processes (Beltrán et al. 2018b). The samples with lower molecular weight have shorter polymer chains, which decompose at lower temperatures, negatively affecting the thermal stability. The presence of the fibroin nanoparticles is positive, because they lead to slight increases in the thermal stability of the recycled plastic, especially in PLAR. To understand this behavior, one should consider the barrier effect of the nanoparticles dispersed in the polymer matrix, which hinder the liberation of the decomposition products and increase the thermal stability of the samples. Furthermore, Patwa et al. (Patwa et al. 2018) reported that SFN restricts the thermal motion of the polymer chains. Finally, Table 3 shows that all the PLAR-chitosan samples, with the exception of PLAR-1LCh, have a thermal stability lower than PLAR. These results could be explained by the variations of the molecular weight observed by means of intrinsic viscosity measurements. Regarding the PLAH-chitosan samples, the effect

Table 2 DSC results (second heating scan) of the PLA-based materials

Sample	T_g (°C)	T_{cc} (°C)	T_m (°C)	ΔH_{cc} (J/g)	ΔH_m (J/g)
PLAV	58.4	112.8	147.8	25.2	26.6
PLAR	58.5	109.9	147.3–153.0	28.2	28.7
PLAH	56.8	106.1	146.3–154.3	33.3	36.2
PLAR-1HSFN	58.1	109.1	147.2–153.9	27.0	28.0
PLAH-1HSFN	57.7	104.4	146.5–154.7	32.2	33.4
PLAR-1DSFN	58.4	109.0	147.1–153.7	27.4	28.2
PLAR-2DSFN	58.4	107.6	147.0–154.0	26.8	27.6
PLAH-1DSFN	57.7	104.4	146.5–154.7	32.2	33.4
PLAR-1LCh	58.5	109.1	147.2–153.5	25.3	25.9
PLAR-5LCh	57.7	107.7	146.6–154.2	29.4	29.8
PLAH-1LCh	57.6	106.7	146.4–154.4	32.2	35.0
PLAH-5LCh	57.8	107.5	146.7–154.7	28.3	30.2
PLAR-1HCh	58.4	106.3	146.6–154.2	29.2	29.4
PLAR-5HCh	57.2	106.6	146.7–154.4	31.1	31.5
PLAH-1HCh	57.6	107.5	146.8–154.6	31.4	32.2

Table 3 TGA characteristic temperatures of PLA-based materials

Sample	T_{10} (°C)	T_{max} (°C)
PLAV	335.4	369.1
PLAR	327.6	367.5
PLAH	325.9	364.5
PLAR-1HSFN	334.3	367.0
PLAH-1HSFN	325.1	361.4
PLAR-1DSFN	331.5	370.1
PLAR-2DSFN	328.2	366.6
PLAH-1DSFN	326.2	361.9
PLAR-1LCh	330.8	365.6
PLAR-5LCh	316.7	360.5
PLAH-1LCh	326.8	365.2
PLAH-5LCh	322.7	361.2
PLAR-1HCh	304.9	352.7
PLAR-5HCh	313.2	357.0
PLAH-1HCh	318.8	359.1

of the low molecular weight chitosan on the thermal stability of PLA is relatively small, while the high molecular chitosan caused a decrease of the thermal stability of the sample.

Mechanical properties of the PLA-based materials

The mechanical properties of the recycled plastics play a very important role in their possible applications in automotive, agriculture, and packaging industries. The effect of the SFN and chitosan on the Vickers hardness of the recycled PLA was studied by means of microhardness measurements, and the results are summarized in Fig. 6. It can be seen that the differences between the various samples are small. Nevertheless, there are some results that might be worth of interest. First of all, Fig. 6 shows that the different aging processes and the reprocessing step caused a decrease on the hardness of PLA samples. This result can be attributed to the degradation of PLA, since the strength and rigidity of a polymer depend on its average molecular weight.

With respect to the effect of the different fillers, it can be seen that the addition of the silk fibroin nanoparticles results in a slight increase of the hardness of the materials. This outcome is especially striking for the PLAR-1HSFN sample, since the intrinsic viscosity values show that the presence of the nanoparticle led to some degradation of PLA. However, the increase of the hardness of the recycled PLA samples can be explained by the fact that SFN acts as a reinforcement of the PLA matrix. Similar findings were reported by Patwa et al. (Patwa et al. 2018), who observed an increase of the elastic modulus, tensile strength, toughness, and Shore D hardness in nanocomposites of virgin PLA with up to 2% of SFN.

In the case of the chitosan-filled samples, it can be seen that the addition of chitosan has a small effect on the Vickers hardness, despite the degradation observed in the samples of postconsumer PLA and high molecular weight chitosan. This behavior suggests that chitosan, especially that of high molecular weight, has two counteracting effects on the hardness of PLA. On the one hand, the degradation caused by chitosan should lead to a decrease of the hardness of the material. On the other hand, chitosan particles seem to have a reinforcement effect, increasing the hardness and counteracting the negative effect of the degradation. The overall result of these opposite effects is that no important changes are observed in the obtained hardness of the polymer.

Gas barrier properties of the PLA-based materials

In the field of packaging applications, especially in that of food products, the gas barrier properties play a very important role. Hence, it is crucial to study the effect of the different organic fillers on the gas barrier properties of mechanically recycled PLA. Figures 7 and 8 present the results obtained for the permeability against O_2, measured in Barrer (1 g·cm/s·cm^2·bar), and the water vapor transmission rate, respectively.

As it can be observed in Fig. 7, recycling does not seem to have a significant effect on the permeability coefficient of oxygen, despite the reduction of the intrinsic viscosity. Similar results were reported in a previous study and were attributed to the dependence of the permeability on two parameters, namely, the gas solubility and the diffusion coefficient (Beltrán et al. 2018b). These parameters are affected by the free volume and structure of the polymer, the size and

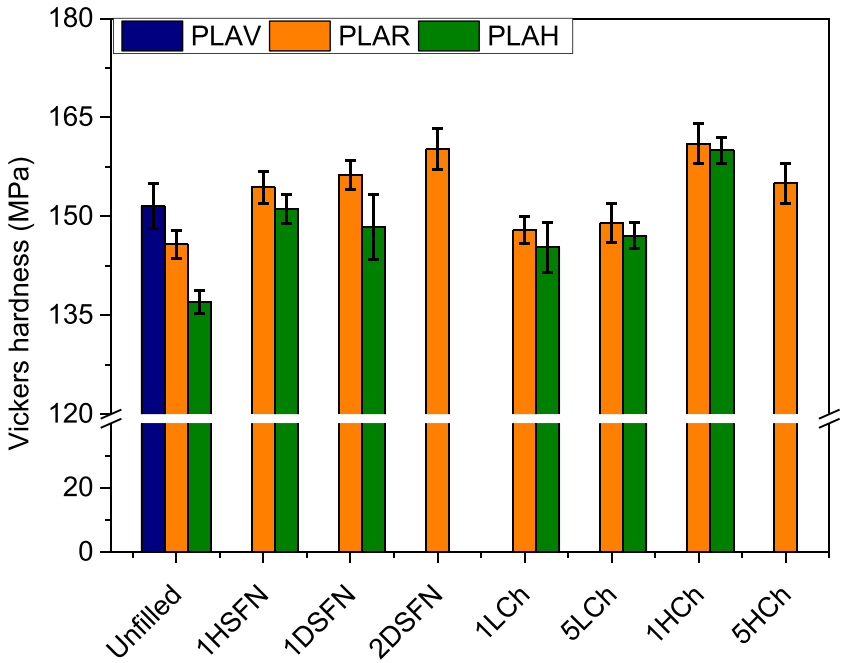

Fig. 6 Vickers hardness of the PLA-based materials

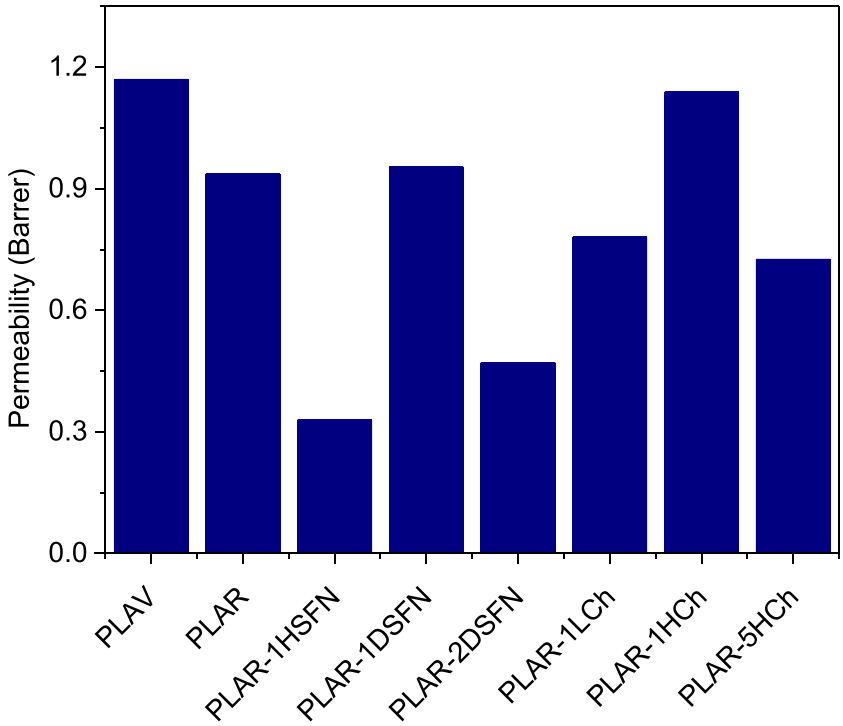

Fig. 7 Oxygen permeability of PLA-based materials

chemical nature of the gas molecules and temperature. Mechanical degradation could lead to a decrease of the diffusion coefficient, since shorter polymer chains can rearrange themselves better, reducing the free volume inside the polymer. On the contrary, the aging, washing, and reprocessing steps lead to an increase of the –COOH and –OH terminal groups, which could increase the affinity between the polymer and the gas molecules, increasing the solubility (Choudalakis and Gotsis 2009). The presence of these two counteracting effects results in the small difference between PLAV and PLAR observed in Fig. 7.

Figure 7 reveals, however, some noteworthy results regarding the effect of the fibroin nanoparticles. Firstly, it can be seen that the addition of HSFN leads to the reduction of the permeability coefficient of O_2, despite the degradation caused by this filler. This result could be attributed to the barrier effect of the nanoparticles dispersed in the polymer matrix, which increase the tortuosity of the diffusion path traveled by the gas

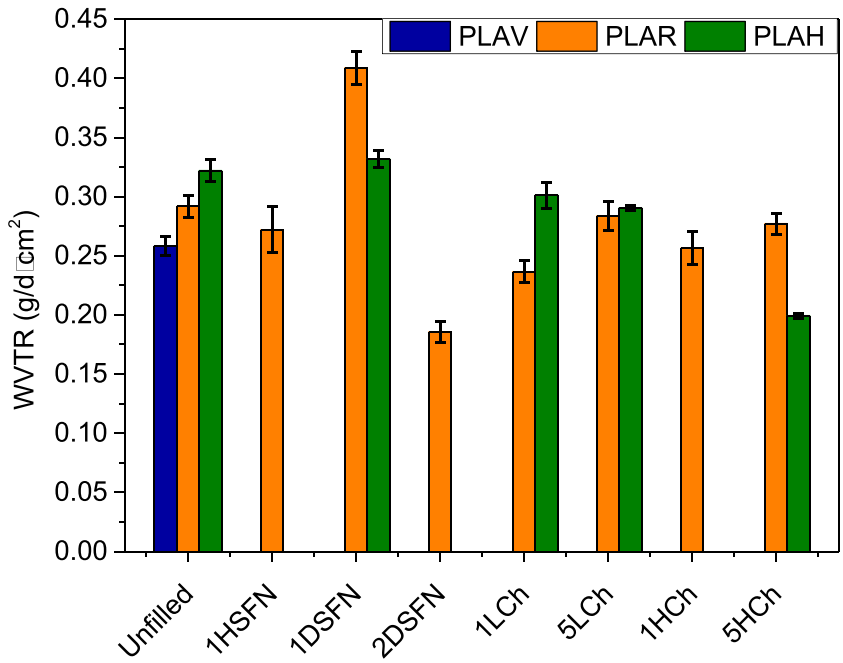

Fig. 8 WVTR of the PLA-based materials

molecules and decrease the permeability of the material. In the case of the samples with DSFN, a larger concentration of nanoparticles was needed to obtain a reduction of the permeability. This behavior could be explained by the worst interaction between DSFN and PLA, observed in SEM microscopy. The poorer dispersion of the DSFN reduces the barrier effect of the nanoparticles, making necessary to add more nanoparticles to decrease the permeability.

As for PLA-chitosan samples, the effect of the filler depends on the molecular weight of the chitosan. In the samples with low molecular weight chitosan, small amounts of the filler lead to a slight decrease of the permeability, probably due to the increase of the viscosity and subsequent reduction of the free volume in the material. However, it is worth to note that the PLAR with 5% low molecular weight chitosan presented a permeability coefficient over 7 Barrer (not shown in Fig. 7). This behavior is probably due to the poor dispersion of the low molecular weight chitosan particles in the PLA matrix. Meanwhile, the samples containing high molecular weight chitosan show a more moderated effect, despite the decrease observed in the intrinsic viscosity. This result might be an indicative of two counteracting effects of the addition of chitosan. On the one hand, the degradation of PLA leads to a larger free volume and thus an increased permeability. On the other hand, high molecular weight chitosan particles have a barrier effect, hindering the gas diffusion through the plastic material.

Figure 8 summarizes the results obtained for the WVTR of the different PLA-based materials. For the unfilled materials, it can be seen that the water vapor transmission rate slightly increases in PLAR and, especially, in PLAH. This behavior might be explained by the presence of a larger amount of terminal –COOH and –OH groups in the recycled materials, which increase the interactions with the water. Such increase in the interactions also increases the diffusion of the water vapor through the polymer films.

With regard to the effect of the silk fibroin nanoparticles, Fig. 8 shows that both HSFN and DSFN are able to reduce the WVTR of recycled PLA, reaching values even lower than that of PLAV. As in the case of the O_2 permeability, the reduction of the WVTR is due to the increase of the tortuosity of the diffusion path as a result of the dispersion of the nanoparticles in the polymer matrix. It is important to point out that a greater amount of DSFN is needed to decrease the WVTR due to the aforementioned lower PLA-DSFN interactions and overall poorer dispersion of DSFN.

Concerning the samples with chitosan, it can be seen in Fig. 8 that the effect of both low molecular weight and high molecular weight chitosan is small. This result might seem rather surprising, since it is expected that the WVTR of the PLA-chitosan samples might increase, due to the hydrophilicity of the chitosan (Bonilla et al. 2013). However, the obtained results agree with those of O_2 permeability, indicating that the dispersed chitosan phase has a certain barrier effect, slowing down the diffusion through the polymer films. In the conditions used in this study, the barrier effect seems to prevail over the hydrophilicity of chitosan, resulting in a slight decrease of WVTR in the PLA-chitosan samples.

In summary, the above findings indicate that the addition of organic fillers leads to a mechanically recycled PLA with improved properties. These results suggest, therefore, that organic fillers are interesting alternatives for upgrading mechanically recycled PLA due to their availability and their renewable origin, which should contribute to lowering the environmental impact of using PLA. However, special attention should be paid to the nature and amount of filler employed, since some properties could be negatively affected.

Conclusions

The effect of adding silk fibroin nanoparticles and chitosan on key properties in packaging applications of recycled PLA was studied. The starting granulated PLA was subjected to two different aging protocols and then melt reprocessed in conjunction either with silk fibroin nanoparticles, prepared by two different methods, or chitosan of low and high molecular weight. The different aging protocols along with the degradation suffered during the melt reprocessing led to a decrease of the intrinsic viscosity, Vickers hardness, thermal stability, and an increase in the permeability of the recycled polymer. Regarding the structure of the recycled materials with organic fillers, SEM analysis shows that, overall, a good dispersion of the different fillers in the polymer matrix was achieved. The effect of the organic fillers on the viscosity varies with the kind of the filler used and the degradation level of PLA. In recycled PLA obtained from slightly degraded PLA, the addition of fibroin obtained by acid hydrolysis and high molecular weight chitosan led to some degradation of the polymer, while in the recycled PLA obtained from severely hydrolyzed plastic, the intrinsic viscosity increased with all the fillers. Despite the degradation of PLA, both silk fibroin nanoparticles and, to a lesser extent, chitosan have a reinforcing effect on mechanically recycled PLA. The addition of carefully selected organic fillers led to an improvement of the thermal stability, mechanical properties, and especially the barrier properties, which are of key importance for packaging applications.

Hence, the addition of these organic fillers represents a potential cost-effective and environmentally sound method for improving the properties of mechanically recycled PLA, which might favor its recyclability, allowing to reduce the consumption of raw materials and contribute to a circular economy approach.

Acknowledgments The authors would like to thank the Institute of Polymer Science and Technology (Madrid, Spain), for collaborating in the SEM measurements.

Funding information This work was supported by MINECO-Spain (project CTM2017-88989-P), Universidad Politécnica de Madrid (project UPM RP 160543006), and the European Commission (Horizon 2020, project 860407-BIO-PLASTICS EUROPE). Dr. Lozano-Pérez's research contract at IMIDA was partially supported (80%) by the ERDF/FEDER Operational Programme "Murcia" CCI N° 2007ES161PO001 (Project No. 14-20/20).

References

Ajisawa A (1998) Dissolution of silk fibroin with calciumchloride/ethanol aqueous solution; studies on the dissolution of silk fibroin. (IX). J Sericult Sci Jpn 67:91–94

Altman GH, Diaz F, Jakuba C, Calabro T, Horan RL, Chen J, Lu H, Richmond J, Kaplan DL (2003) Silk-based biomaterials. Biomaterials 24:401–416

Auras R, Lim L, Selke SEM, Tsuji H (2010) Poly(lactic acid): synthesis, structures, properties, processing, and applications. John Wiley & Sons, Hoboken

Beltrán FR, Lorenzo V, de la Orden MU, Martínez-Urreaga J (2016) Effect of different mechanical recycling processes on the hydrolytic degradation of poly(l-lactic acid). Polym Degrad Stab 133:339–348

Beltrán FR, Ortega E, Solvoll AM, Lorenzo V, de la Orden MU, Martínez Urreaga J (2018a) Effects of aging and different mechanical recycling processes on the structure and properties of poly(lactic acid)-clay nanocomposites. J Polym Environ 26:2142–2152

Beltrán FR, Lorenzo V, Acosta J, de la Orden MU, Martínez Urreaga J (2018b) Effect of simulated mechanical recycling processes on the structure and properties of poly(lactic acid). J Environ Manag 216:25–31

Beltrán FR, de la Orden MU, Martínez Urreaga J (2018c) Amino-modified halloysite nanotubes to reduce polymer degradation and improve the performance of mechanically recycled poly(lactic acid). J Polym Environ 26:4046–4055

Beltrán FR, Infante C, de la Orden MU, Martínez Urreaga J (2019) Mechanical recycling of poly(lactic acid): evaluation of a chain extender and a peroxide as additives for upgrading the recycled plastic. J Clean Prod 219:46–56. https://doi.org/10.1016/j.jclepro.2019.01.206

Bonilla J, Fortunati E, Vargas M, Chiralt A, Kenny JM (2013) Effects of chitosan on the physicochemical and antimicrobial properties of PLA films. J Food Eng 119:236–243

Castro-Aguirre E, Iñiguez-Franco F, Samsudin H, Fang X, Auras R (2016) Poly(lactic acid)—mass production, processing, industrial applications, and end of life. Adv Drug Deliv Rev 107:333–366

Cecchi T, Giuliani A, Iacopini F, Santulli C, Sarasini F, TirillÃ J (2019) Unprecedented high percentage of food waste powder filler in poly lactic acid green composites: synthesis, characterization, and volatile profile. Environ Sci Pollut Res 26:7263–7271

Chinthapalli R, Skoczinski P, Carus M, Baltus W, de Guzman D, Käb H, Raschka A, Ravenstijn J (2019) Bio-based building blocks and polymers – global capacities, production and trends 2018–2023. nova-Institut GmbH, Germany

Choudalakis G, Gotsis AD (2009) Permeability of polymer/clay nanocomposites: a review. Eur Polym J 45:967–984

Cuadri AA, Martín-Alfonso JE (2018) Thermal, thermo-oxidative and thermomechanical degradation of PLA: a comparative study based on rheological, chemical and thermal properties. Polym Degrad Stab 150:37–45

Di Lorenzo ML (2006) Calorimetric analysis of the multiple melting behavior of poly(L-lactic acid). J Appl Polym Sci 100:3145–3151

Elsawy MA, Saad GR, Sayed AM (2016) Mechanical, thermal, and dielectric properties of poly(lactic acid)/chitosan nanocomposites. Polym Eng Sci 56:987–994

Elsawy MA, Kim K, Park J, Deep A (2017) Hydrolytic degradation of polylactic acid (PLA) and its composites. Renew Sust Energ Rev 79:1346–1352

Farah S, Anderson DG, Langer R (2016) Physical and mechanical properties of PLA, and their functions in widespread applications — a comprehensive review. Adv Drug Deliv Rev 107:367–392

Haider T, Völker C, Kramm J, Landfester K, Wurm FR (2018) Plastics of the future? The impact of biodegradable polymers on the environment and on society. Angew Chem Int Ed. https://doi.org/10.1002/anie.201805766

Hijazi N, Le Moigne N, Rodier E, Sauceau M, Vincent T, Benezet J, Fages J (2019) Biocomposite films based on poly(lactic acid) and chitosan nanoparticles: elaboration, microstructural and thermal characterization. Polym Eng Sci 59:E350–E360

Li W, Sun Q, Mu B, Luo G, Xu H, Yang Y (2019) Poly(l-lactic acid) biocomposites reinforced by oligo(d-lactic acid) grafted chitosan for simultaneously improved ductility, strength and modulus. Int J Biol Macromol 131:495–504

Lozano-Pérez AA, Rivero HC, Pérez Hernández MDC, Pagán A, Montalbán MG, Víllora G, Cénis JL (2017) Silk fibroin nanoparticles: efficient vehicles for the natural antioxidant quercetin. Int J Pharm 518:11–19

Mülhaupt R (2013) Green polymer chemistry and bio-based plastics: dreams and reality. Macromol Chem Phys 214:159–174

Nagarajan V, Mohanty AK, Misra M (2016) Perspective on polylactic acid (PLA) based sustainable materials for durable applications: focus on toughness and heat resistance. ACS Sustain Chem Eng 4:2899–2916

Niaounakis M (2019) Recycling of biopolymers – the patent perspective. Eur Polym J 114:464–475

Omenetto FG, Kaplan DL (2010) New opportunities for an ancient material. Science 329:528–531. https://doi.org/10.1126/science.1188936

Patwa R, Kumar A, Katiyar V (2018) Effect of silk nano-disc dispersion on mechanical, thermal, and barrier properties of poly(lactic acid) based bionanocomposites. J Appl Polym Sci 135:46671

Reddy MM, Vivekanandhan S, Misra M, Bhatia SK, Mohanty AK (2013) Biobased plastics and bionanocomposites: current status and future opportunities. Prog Polym Sci 38:1653–1689

Rossi V, Cleeve-Edwards N, Lundquist L, Schenker U, Dubois C, Humbert S, Jolliet O (2015) Life cycle assessment of end-of-life options for two biodegradable packaging materials: sound application of the European waste hierarchy. J Clean Prod 86:132–145

Soroudi A, Jakubowicz I (2013) Recycling of bioplastics, their blends and biocomposites: a review. Eur Polym J 49:2839–2858

Suyatma NE, Copinet A, Tighzert L, Coma V (2004) Mechanical and barrier properties of biodegradable films made from chitosan and poly (lactic acid) blends. J Polym Environ 12:1–6

Tao Y, Xu W, Yan Y, Cao Y (2012) Preparation and characterization of silk fibroin nanocrystals. Polym Int 61:760–767

Tesfaye M, Patwa R, Gupta A, Kashyap MJ, Katiyar V (2017) Recycling of poly (lactic acid)/silk based bionanocomposites films and its influence on thermal stability, crystallization kinetics, solution and melt rheology. Int J Biol Macromol 101:580–594

Zhao P, Rao C, Gu F, Sharmin N, Fu J (2018) Close-looped recycling of polylactic acid used in 3D printing: an experimental investigation and life cycle assessment. J Clean Prod 197:1046–1055

Zhou C, Confalonieri F, Jacquet M, Perasso R, Li Z, Janin J (2001) Silk fibroin: structural implications of a remarkable amino acid sequence. Proteins 44:119–122